
Why GRPO Needs Normalization: A Local-Curvature Perspective on Adaptive Gradients

Cheng Ge ^{*1} Caitlyn Heqi Yin ^{*2} Hao Liang ^{†3} Jiawei Zhang ^{†4}

Abstract

Reinforcement learning (RL) has become a key driver of language model reasoning. Among RL algorithms, Group Relative Policy Optimization (GRPO) is the de facto standard, avoiding the need for a critic by using per-prompt baselines and variance normalization. Yet why and when this normalization helps remains unclear. In this work, we provide an explanation through the lens of local curvature of the sequence-level policy gradient: standard deviation normalization implements an adaptive gradient. Theoretically, under mild conditions, GRPO enjoys a strictly improved convergence rate over unnormalized REINFORCE, with gains characterized by the average within-prompt reward standard deviation across prompts and iterations. Empirically, our analysis on GSM8K and MATH benchmarks reveals three distinct training phases governed by the interplay between feature orthogonality and reward variance: (I) an early acceleration phase where high variance and orthogonality favor adaptive scaling; (II) a relatively stable transition phase; and (III) a late-stage regime where the loss of orthogonality limits further gains. Together, these results provide a principled account of when std normalization helps in GRPO, and offer broader insights into the design of critic-free RL algorithms.

1. Introduction

Large language models (LLMs) have recently exhibited striking gains in multi-step reasoning, particularly when a

^{*}Equal contribution; authors are listed in alphabetical order.
[†]co-last authors ¹Department of Aeronautics and Astronautics, MIT ²Department of Statistics, University of Wisconsin–Madison ³Department of Informatics, King’s College London ⁴Department of Computer Sciences, University of Wisconsin–Madison. Correspondence to: Hao Liang <haoliang.research@gmail.com>, Jiawei Zhang <jzhang2924@wisc.edu>.

lightweight reinforcement-learning (RL) stage is applied on top of a strong and pretrained base model. Among the many post-training recipes, Group Relative Policy Optimization (GRPO) has emerged as a practical, critic-free alternative that has powered some of the most visible reasoning systems (Shao et al., 2024), where it consistently improves solution accuracy under tight compute budgets.

While Proximal Policy Optimization (PPO) (Schulman et al., 2017) remains a popular default in RLHF pipelines, it couples the policy with a learned value-function critic (and often GAE (Schulman et al., 2015)). This increases memory footprint and implementation complexity, since the environment is a pretrained LLM and rewards arrive only at the end of whole sequences. This has renewed interest in critic-free policy-gradient methods that operate at the sequence level, such as REINFORCE-style method, including ReMax (Li et al., 2023), and RLOO (Ahmadian et al., 2024), which often match or outperform PPO for LLM alignment while being simpler and lighter-weight.

Classical REINFORCE (Williams, 1992) reduces gradient variance by subtracting a baseline (e.g., a running mean reward), yielding an unbiased estimator with lower variance (Greensmith et al., 2004). This is textbook policy-gradient variance reduction. GRPO goes one step further: for each prompt, it samples multiple responses from the current policy, computes the group mean reward as a baseline, and normalizes each response’s update by the within-prompt reward standard deviation, which effectively uses a per-prompt z-scored advantage (Shao et al., 2024). Empirically, this simple normalization has been repeatedly observed to stabilize optimization and improve sample-efficiency in LLM RL (Lambert, 2025). Yet, the underlying mechanism of this normalization step has not been theoretically clarified.

What, exactly, does normalization do? In this work, we provide a principled explanation of why and when GRPO benefits from it. Our key insight is that the reward variance of each question serves as an estimate of the local Lipschitz constant (curvature) of the policy gradient. Standard-deviation normalization therefore implements an adaptive gradient rule, scaling each update by an inverse-curvature proxy and effectively assigning a larger step size to smoother prompts and a smaller step size to sharper prompts. This

mechanism improves stability and convergence precisely when (i) curvature is heterogeneous across prompts and evolves over training, and (ii) cross-prompt interference is controlled so that prompt-wise adaptive steps are not overwhelmed by interaction noise. This perspective explains why GRPO can outperform unnormalized policy gradient methods in practice.

We characterize concrete conditions under which normalization yields gains both theoretically and empirically. To summarize, our contributions are:

- **Curvature interpretation.** We provide a new perspective on GRPO as a principled adaptive gradient mechanism that adapts learning to per-prompt curvature.
- **When normalization provably helps.** We show that under reasonable and mild assumptions, GRPO attains a faster convergence rate than unnormalized REINFORCE, with the speedup explicitly governed by the average per-prompt standard deviation factors over time.
- **When normalization empirically helps and when it saturates.** On GSM8K and MATH, we validate the curvature–variance link and uncover three regimes for normalization: (I) early, near-orthogonal high-variance training where gains can be muted by noisy gradients; (II) a mid-stage with moderate variance and stable interactions where normalization delivers the strongest and most consistent improvements, especially on harder prompts; and (III) a late stage where reduced orthogonality increases interference and the marginal benefit plateaus.

Our results explain why GRPO needs normalization: it is a principled adaptive gradient mechanism whose benefits emerge under identifiable geometric and statistical conditions. This provides a theoretical foundation for the empirical success of GRPO and offers broader insights into the design of critic-free RL algorithms for LLM training.

1.1. Related works

REINFORCE-style PG methods (prior to GRPO). Li et al. (2023) proposes a sequence-level REINFORCE-style algorithm, ReMax, for LLM alignment. Ahmadian et al. (2024) proposes RLOO, which samples multiple responses per prompt and uses a leave-one-out baseline to further reduce variance.

GRPO and its variants. GRPO (Shao et al., 2024) and related methods (Simoni et al., 2025; Liu et al., 2025; Chu et al., 2025; Lin et al., 2025b) have gained widespread adoption due to their simplicity and scalability, and are now commonly used in post-training pipelines for reasoning-oriented models. Several extensions improve stability in long-CoT RL. DAPO (Yu et al., 2025a) introduces several techniques, including higher clipping thresholds and sequence-level

losses, to make the training more stable. GSPO (Zheng et al., 2025) replaces the sequence-level importance weight with sequence likelihood to avoid high-variance noise. CISPO (Chen et al., 2025) further revises the clipping strategy to avoid low-probability tokens from being clipped out after the first on-policy update.

Emerging theory for GRPO. Recent studies analyze what GRPO optimizes and how it behaves in on- and off-policy regimes (Mroueh et al., 2025), its implicit alignment objective (Vojnovic & Yun, 2025), and trajectory-corrected variants with convergence guarantees (Pang & Jin, 2025). Bereket & Leskovec (2025) highlights a trade-off between normalization and calibration, showing that removing the std term can improve probability calibration at the cost of optimization speed. Jain et al. (2025) interprets GRPO’s optimization as a weighted combination of maximization likelihood for correct rollouts and minimization for the incorrect ones, while noting that the use of std normalization lacks a clear theoretical motivation. We contribute a new perspective, interpreting the std term as an adaptive gradient mechanism reflecting local curvature, which helps unify a range of previously disparate empirical findings.

RLVR. Reinforcement learning with verifiable rewards (RLVR) has emerged as an effective paradigm for reasoning-intensive domains. Unlike RLHF, which relies on a learned reward model, RLVR uses deterministic, verifiable rewards (Lambert et al., 2024; Guo et al., 2025; Team et al., 2025; Wang et al., 2025). This mitigates reward-model bias and hacking and simplifies training, while scaling effectively with compute and dataset size. Strong results have been reported on the well-recognized GSM8K (Cobbe et al., 2021), MATH (Hendrycks et al., 2021), Omni-MATH (Gao et al., 2024), and FormalMATH (Yu et al., 2025b). In this paper, we focus on developing a theoretical understanding of GRPO in the RLVR setting.

2. Preliminaries and Problem Settings

We begin by introducing the RLVR framework for LLM training and reviewing the GRPO algorithm, including the policy parametrization and update rules.

Notation. For a finite set \mathcal{X} , we denote by $\Delta(\mathcal{X})$ the set of probability distributions over \mathcal{X} . By default, all vectors are treated as column vectors. $\|\cdot\| = \|\cdot\|_2$ denotes the Euclidean norm for vectors and the spectral norm for matrices. For $v \in \mathbb{R}^m$, we use $\text{diag}(v) \in \mathbb{R}^{m \times m}$ to denote the diagonal matrix with v on its diagonal. We also use the shorthand notation $[m] := \{1, \dots, m\}$ and $\mathcal{B}(v, r) := \{x \in \mathbb{R}^m \mid \|x - v\|_2 \leq r\}$.

We say that a continuously differentiable function f :

$\mathbb{R}^m \rightarrow \mathbb{R}^n$ is C -Lipschitz continuous if $\|\nabla f(x)\| \leq C$ for all $x \in \mathbb{R}^m$. A function $f : \mathbb{R}^n \rightarrow \mathbb{R}$ is said to be ρ -weakly convex over $\mathcal{B}(v, r)$ if $f + \frac{\rho}{2}\|\cdot\|^2$ is convex over $\mathcal{B}(v, r)$. Moreover, f is L -smooth over $\mathcal{B}(v, r)$ if for all $x_1, x_2 \in \mathcal{B}(v, r)$, $\|\nabla f(x_1) - \nabla f(x_2)\| \leq L\|x_1 - x_2\|$. An L -smooth function over $\mathcal{B}(v, r)$ is automatically L -weakly convex on the same set. Throughout the paper, we do not distinguish between a Lipschitz-smooth function and a function with Lipschitz-continuous gradients, nor do we differentiate among the smoothness constant, the Lipschitz constant of the gradient, and the curvature. Finally, we use the terms question (answer) and prompt (output) interchangeably.

2.1. Problem Setup

RLVR. We consider a sequence-level RL with verifiable reward (RLVR) framework for training LLMs. RLVR (Lambert et al., 2024; Guo et al., 2025; Team et al., 2025; Wang et al., 2025) has recently emerged as an effective paradigm for improving LLM reasoning performance, particularly in domains with deterministic and automatically verifiable rewards. Let $\mathcal{Q} = \{q_1, \dots, q_n\}$ denote the set of questions and $\mathcal{O} = \{o_1, \dots, o_K\}$ the set of possible output sequences. A predefined deterministic reward function $r : \mathcal{Q} \times \mathcal{O} \rightarrow \{0, 1\}$ evaluates the correctness of a response, where $r(q, o) = 1$ if the o is a correct response to q , and $r(q, o) = 0$ otherwise. Given a question q , the LLM generates a response $o \sim \pi_\theta(q)$ according to a stochastic policy $\pi_\theta : \mathcal{Q} \rightarrow \Delta(\mathcal{O})$, parameterized by $\theta \in \Theta$. The objective is to learn a policy that maximizes the expected reward over the question set:

$$J(\theta) := \frac{1}{n} \sum_{i=1}^n J_i(\theta) = \frac{1}{n} \sum_{i=1}^n \mathbb{E}_{o \sim \pi_\theta(\cdot|q_i)} [r(o, q_i)], \quad (1)$$

where $J_i(\theta) := \mathbb{E}_{o \sim \pi_\theta(\cdot|q_i)} [r(o, q_i)]$ denotes the expect reward of policy π_θ on question q_i .

Remark 2.1. In LLM alignment settings such as RLHF, an additional KL penalty term is often introduced to mitigate over-optimization of the reward model:

$$J_{\text{KL}}(\theta) := \frac{1}{n} \sum_{i=1}^n \mathbb{E}_{o \sim \pi_\theta(\cdot|q_i)} [r(o, q_i)] - \beta \text{KL}(\pi_\theta \| \pi_{\text{ref}}),$$

where $\beta \geq 0$ is the regularization parameter and π_{ref} denotes a reference policy (Shao et al., 2024). In contrast, for RLVR, recent studies (Chu et al., 2025; Hu et al., 2025) have shown that removing the KL term can yield faster convergence and improved performance. Consequently, throughout this paper we focus on the unregularized objective, where $J_{\text{KL}}(\theta)$ reduces to $J(\theta)$ in Equation 1 for $\beta = 0$.

In this paper, we consider an on-policy setting with *exact* gradient and randomly selected questions. At each iteration, a question q_i is sampled *uniformly* from \mathcal{Q} , and the corresponding gradient $\nabla J_i(\theta)$ is evaluated exactly.

PPO. PPO (Schulman et al., 2017) has become a standard baseline for LLM alignment due to its stability and empirical effectiveness (Ouyang et al., 2022; Rafailov et al., 2023). By combining policy gradient updates with a learned value-function critic and a clipped surrogate objective, PPO mitigates large policy updates and improves training robustness. Its objective function of PPO is given by:

$$J_{\text{PPO}}(\theta) = \frac{1}{n} \sum_{i=1}^n \mathbb{E}_{o \sim \pi_{\theta_{\text{old}}}(\cdot|q_i)} \left[\min \left(\gamma_i(o) A_i(o), \text{clip}(\gamma_i(o), 1 - \epsilon, 1 + \epsilon) A_i(o) \right) \right], \quad (2)$$

where $\epsilon \in (0, 1)$ is the clipping parameter, and $\gamma_i(o) := \frac{\pi_\theta(o|q_i)}{\pi_{\theta_{\text{old}}}(o|q_i)}$ is the importance ratio between the current policy π_θ and the old policy $\pi_{\theta_{\text{old}}}$. The advantage $A_i(o)$ is calculated using Generalized Advantage Estimation with a learned critic. However, the reliance on a critic introduces additional computational overhead and implementation complexity. These considerations have motivated growing interest in critic-free alternatives such as REINFORCE.

REINFORCE. Unlike PPO, REINFORCE (Williams, 1992) appears well-suited for LLM alignment as it efficiently estimates the gradient with a single query of the language and reward model. It does not require training a value model, making it computationally more efficient than PPO. However, REINFORCE is known to suffer from high variance in its stochastic gradient estimates (Li et al., 2023). In this paper, we focus on the *exact* setting where the full gradient is computed for randomly selected questions. Under this setting, all critic-free policy gradient methods, including REINFORCE, reduce to the vanilla policy gradient update, as summarized in Algorithm 1.

Algorithm 1 Critic-free Policy Gradient Method

```

Input: learning rate  $\eta > 0$ , initial parameter  $\theta_0$ .
for  $t = 1$  to  $T$  do
    Select  $i_t$  uniformly at random from  $\{1, \dots, n\}$ 
     $\theta_t \leftarrow \theta_{t-1} + \eta \nabla J_{i_t}(\theta_{t-1})$ 
end for
Return: final policy  $\pi_{\theta_{T-1}}$ 

```

2.2. GRPO

GRPO, introduced in DeepSeek-Math (Shao et al., 2024) and DeepSeek-R1 (Guo et al., 2025), builds on the computational efficiency of REINFORCE by eliminating the learned value-function critic while substantially improving empirical performance. The GRPO objective closely resembles

the PPO objective in Equation (2):

$$\frac{1}{n} \sum_{i=1}^n \mathbb{E}_{o \sim \pi_{\theta_{\text{old}}}(\cdot | q_i)} \left[\min \left(\gamma_i(o) A_i(o), \right. \right. \\ \left. \left. \text{clip}(\gamma_i(o), 1 - \epsilon, 1 + \epsilon) A_i(o) \right) \right], \quad (3)$$

differing only in the advantage term $A_i(o)$. Specifically, GRPO defines the advantage as:

$$A_i(o) := \frac{r(q_i, o) - \mathbb{E}_{o' \sim \pi_{\theta_{\text{old}}}(\cdot | q_i)} [r(q_i, o')]}{\sqrt{\mathbb{V}_{o' \sim \pi_{\theta_{\text{old}}}(\cdot | q_i)} [r(q_i, o')]}} ,$$

which uses the group mean reward as a baseline, and normalizes each update by the within-prompt reward standard deviation. For theoretical analysis, we impose the assumption that each question admits a unique correct answer, a condition commonly adopted in the study of RL algorithms (Mei et al., 2020; 2023; Lin et al., 2025a).

Assumption 1 (Unique correct answer). For any $q \in \mathcal{Q}$, there exists a unique $o^*(q) \in \mathcal{O}$ such that $r(q, o^*(q)) = 1$.

Under Assumption 1, let a_i denote the index of the correct answer for question $q_i \in \mathcal{Q}$, so that $r(q_i, o_{a_i}) = 1$. We use $r_i \in \mathbb{R}^K$ to denote the *one-hot* reward vector for question q_i , with $[r_i]_j = r(q_i, o_j), \forall j \in [K]$. We consider the on-policy scenario where $\pi_{\theta} = \pi_{\theta_{\text{old}}}$. Let $\pi_{\theta}^*(i) := \pi_{\theta}(o_{a_i} | q_i)$ be the success probability of policy π_{θ} on question q_i , and let $\mathbb{V}[\pi_{\theta}(i)] = \pi_{\theta}^*(i)(1 - \pi_{\theta}^*(i))$ denote its Bernoulli reward variance. Under this setting, the importance ratio $\gamma_i(o) = 1$, and the GRPO advantage simplifies to

$$A_i(o) = \frac{r(q_i, o) - \text{sg}(\pi_{\theta}^*(i))}{\text{sg}(\sqrt{\mathbb{V}[\pi_{\theta}(i)]})}, \quad (4)$$

where $\text{sg}(\cdot)$ denotes the stop-gradient operator, which treats its argument as a constant during backpropagation. The GRPO objective can be simplified as:

$$J_{\text{GRPO}}(\theta) = \frac{1}{n} \sum_{i=1}^n J_{\text{GRPO}}^i(\theta) := \frac{1}{n} \sum_{i=1}^n \mathbb{E}_{o \sim \pi_{\theta}} [A_i(o)].$$

We further denote by $\pi_{\theta}(i) \in \mathbb{R}^K$ the probability vector for π_{θ} on question i , with $[\pi_{\theta}(i)]_j := \pi_{\theta}(o_j | q_i), \forall j \in [K]$. Since subtracting a constant baseline does not affect the gradient of the objective, we therefore refer to the resulting algorithm as *(on-policy) GRPO*. Our key observation is that the variance normalization in GRPO implicitly implements an adaptive step size. In particular, for all $i \in [n]$,

$$\nabla J_{\text{GRPO}}^i(\theta) = \mathbb{E}_{o \sim \pi_{\theta}} [A_i(o) \nabla \ln \pi_{\theta}(o | q_i)] \\ = \frac{\mathbb{E}_{o \sim \pi_{\theta}} [r(q_i, o) \nabla \ln \pi_{\theta}(o | q_i)]}{\sqrt{\mathbb{V}[\pi_{\theta}(i)]}} \\ = \frac{\nabla J_i(\theta)}{\sqrt{\mathbb{V}[\pi_{\theta}(i)]}}. \quad (5)$$

The first and last equalities follow from the policy gradient theorem (Sutton et al., 1998). The second equality holds because subtracting a constant baseline does not affect the gradient calculation. The pseudo-code for GRPO is provided in Algorithm 2.

Policy parametrization. We focus on the *log-linear policy parametrization*, which has been widely studied in the analysis of policy gradient methods (Agarwal et al., 2021; Yuan et al., 2022). Specifically, for each question-output pair (q_i, o_j) , we assume the existence of a fixed feature vector $x_{i,j} \in \mathbb{R}^d$, and define the policy as

$$\pi_{\theta}(o_j | q_i) := \frac{\exp(x_{i,j}^{\top} \theta)}{\sum_{l=1}^K \exp(x_{i,l}^{\top} \theta)}. \quad (6)$$

We denote by $X_i \in \mathbb{R}^{K \times d}$ the feature matrix associated with question q_i : $X_i := (x_{i,1}, \dots, x_{i,K})^{\top}$. The explicit update rules for REINFORCE (Algorithm 1) and GRPO (Algorithm 2) under this parametrization are provided in Appendix B.

Algorithm 2 On-policy GRPO

Input: learning rate $\eta > 0$, initial parameter θ_0 .
for $t = 1$ to T **do**
 Select i_t uniformly at random from $\{1, \dots, n\}$
 $\theta_t \leftarrow \theta_{t-1} + \eta \frac{\nabla J_{i_t}(\theta_{t-1})}{\sqrt{\pi_{\theta_{t-1}}^*(i_t)(1 - \pi_{\theta_{t-1}}^*(i_t))}}$
end for
Return: final policy $\pi_{\theta_{T-1}}$

3. Theoretical Results

In this section, we present a convergence analysis of REINFORCE and GRPO. We show that GRPO can achieve provably faster convergence than REINFORCE under our assumptions. It is worth noting that PG with linear function approximation may fail to converge to the optimal policy in general. Accordingly, our analysis focuses on convergence rates toward stationary points.

3.1. Local Smoothness of Objective Function

We begin by relating reward variance to the smoothness of the per-prompt objective. Let $X_{\max} := \max_{i \in [n]} \|X_i\|$.

Lemma 3.1. Under Assumption 1, for all $i \in [n]$ and $\theta \in \mathbb{R}^d$,

$$\|\nabla^2 J_i(\theta)\| \leq 4X_{\max}^2 \cdot \mathbb{V}[\pi_{\theta}(i)], \quad (7)$$

Moreover,

$$\|\nabla^2 J_i(\theta)\| \leq X_{\max}^2, \quad (8)$$

and hence $J_i(\theta)$ is X_{\max}^2 -smooth on \mathbb{R}^d .

The proof is provided in Appendix C.1. This lemma shows that the local smoothness constant of $J_i(\theta)$ is directly controlled by the reward variance of q_i under the current policy π_θ . For deterministic gradient descent on an L -smooth function, a step size of $1/L$ is a standard choice (Garrigos & Gower, 2023). Lemma 3.1 therefore motivates adapting the step size to the local smoothness constant of each per-prompt objective $J_i(\theta)$, which varies across prompts. GRPO achieves exactly this by normalizing updates with reward variance, which implicitly implements an adaptive step size matched to the local curvature of each prompt.

3.2. Orthogonal Representation

To extend this intuition from per-prompt objectives J_i to the averaged objective $J = \frac{1}{n} \sum_i J_i$, we need to control the interactions between different prompts. In particular, we must ensure that gradients associated with prompts do not interfere destructively during optimization. Empirically, as will be shown in Section 4.1, gradients associated with different prompts are nearly orthogonal. Motivated by this observation, we introduce the following assumption to facilitate theoretical analysis.

Assumption 2 (Orthogonal representation). For all $i, j \in [n]$ with $i \neq j$, we have $X_i X_j^\top = 0$.

This assumption ensures that the gradients associated with different prompts are mutually orthogonal, allowing their effects on the optimization dynamics to be analyzed independently for both REINFORCE and GRPO. We further impose the following assumption on the bound of within-prompt Bernoulli variance at every step.

Assumption 3 (Bounded variance). For each $i \in [n]$, there exists a positive sequence $\{C_{i_t}\}_{t=1}^\infty$ such that

$$\sqrt{\mathbb{V}[\pi_{\theta_t}(i)]} \leq C_{i_t} \leq \frac{1}{2}.$$

3.3. Convergence Result under the Orthogonal Representation Assumption

Before presenting the convergence results for Algorithm 1 and 2, we further characterize the smoothness properties of J_i at each iteration.

Lemma 3.2. *Under Assumption 1, for all $i \in [n]$, $J_i(\theta)$ is $\frac{1}{2}X_{\max}$ -Lipschitz over \mathbb{R}^d .*

Lemma 3.3 (Non-uniform local smoothness). *Under Assumption 1, for all $i \in [n]$ and $\theta \in \mathbb{R}^d$, we have $\|\nabla^2 J_i(\theta')\| \leq \frac{5}{2}X_{\max}^2 \cdot \sqrt{\mathbb{V}(\pi_\theta(i))}$ for every $\theta' \in \mathcal{B}(\theta, \frac{1}{X_{\max}} \cdot \sqrt{\mathbb{V}(\pi_\theta(i))})$. Consequently, J_i is $\frac{5}{2}X_{\max}^2 \cdot \sqrt{\mathbb{V}(\pi_\theta(i))}$ -smooth within this neighborhood.*

The proofs are provided in Section C.2 and C.3. We now present our two main theorems, which establish the conver-

gence guarantees for REINFORCE and GRPO, respectively. Their detailed proofs are deferred in Appendix D.

Theorem 3.1 (Convergence rate of REINFORCE). *Under Assumption 1-2, with step size $\eta = \frac{1}{X_{\max}^2}$, we have:*

$$\mathbb{E}[J_i(\theta_t)] - \mathbb{E}[J_i(\theta_{t-1})] \leq -\frac{1}{2nX_{\max}^2} \mathbb{E}[\|\nabla J_i(\theta_{t-1})\|^2].$$

Moreover,

$$\sum_{t=0}^{T-1} \mathbb{E}[\|\nabla J_i(\theta_t)\|^2] \leq 2n(1 - \pi_{\theta_0}^*(i)) X_{\max}^2,$$

Theorem 3.2 (Convergence rate of GRPO). *Under Assumption 1-3 with the step size $\eta = \frac{1}{2X_{\max}^2}$, the following holds:*

$$\mathbb{E}[J_i(\theta_t)] - \mathbb{E}[J_i(\theta_{t-1})] \leq -\frac{3\mathbb{E}[\|\nabla J_i(\theta_{t-1})\|^2]}{16nX_{\max}^2 C_{i_t}},$$

Moreover, we have

$$\sum_{t=0}^{T-1} \mathbb{E}[\|\nabla J_i(\theta_t)\|^2] \leq 2n(1 - \pi_{\theta_0}^*(i)) X_{\max}^2 \cdot C(i, T),$$

$$\text{where } C(i, T) := \frac{8}{3T} \sum_{t=0}^{T-1} C_{i_t}.$$

Proof sketch. The analysis relies on the following key steps.

Step 1: Decoupling across prompts. By the log-linear parametrization and Assumption 2, updates induced by question q_{i_t} lie in a subspace orthogonal to those of any q_l with $l \neq i_t$. Hence, if $i_t \neq l$, then $J_l(\theta_{t+1}) = J_l(\theta_t)$.

Step 2: One-step improvement for the active prompt. When $i_t = l$, choosing an appropriate step size guarantees a sufficient one-step improvement of J_l . For REINFORCE, this follows from the global smoothness bound in Lemma 3.1. For GRPO, the variance-normalized update ensures that $\theta_{t+1} \in \mathcal{B}\left(\theta_t, \frac{1}{X_{\max}} \sqrt{\mathbb{V}(\pi_{\theta_t}(l))}\right)$, where the non-uniform local smoothness in Lemma 3.3 applies.

Taking expectations and summing over iterations yields a telescoping inequality, leading to the stated bounds on the cumulative expected gradient norm. \square

According to Assumption 3, we use $\frac{1}{T} \sum_{i=0}^{T-1} \sqrt{\mathbb{V}[\pi_{\theta_t}(i)]}$ as an estimate of $\frac{1}{T} \sum_{t=0}^{T-1} C_{i_t}$ in Theorem 3.2. Comparing Theorems 3.1 and 3.2, we observe that GRPO achieves a strictly better average convergence bound than REINFORCE, provided that the following constant factor satisfies

$$C(T) := \sum_{i=1}^n \frac{8}{3nT} \sum_{j=0}^{T-1} \sqrt{\mathbb{V}(\pi_{\theta_j}(i))} < 1.$$

Here, $C(T)$ represents the average of the within-prompt Bernoulli standard deviation over both prompts i and iterations. In practice, $C(T)$ is typically much smaller than 1 when the question set contains heterogeneous prompts with varying levels of difficulty. Intuitively, GRPO automatically assigns smaller effective step sizes to prompts with higher curvature, yielding faster convergence on average. Similar improvements can also be expected in settings where the curvature varies significantly across iterations.

3.4. Convergence under Relaxed Assumptions

While the orthogonal representation assumption enables clean decoupling between prompts, empirical results shown in Section 4.1 suggest that gradients associated with different prompts are only *approximately* orthogonal rather than exactly so. In realistic LLM training, prompt representations exhibit small but non-zero cosine similarities, indicating weak yet non-negligible interactions between per-prompt updates. To deal with this more realistic regime, we introduce a relaxed set of assumptions that control these cross-prompt interactions.

Assumption 4 (Bounded cross-prompt interaction). There exists a positive constant M such that for all $i \neq j \in [n]$,

$$M \langle \nabla J_i(\theta_t), \nabla J_j(\theta_t) \rangle \geq \frac{\|X_i \nabla J_j(\theta_t)\|^2}{\|X_i\|^2}.$$

Assumption 4 ensures that cross-prompt gradient interactions are well controlled. The inner product between gradients is positive and upper-bounds the squared projection of $\nabla J_j(\theta_t)$ onto the representation subspace for prompt i . When representations are orthogonal, both sides of the inequality vanish, and the assumption holds trivially.

To prevent any single prompt from dominating the optimization dynamics, we impose a scale-regularity condition.

Assumption 5 (Scale regularity). There exists positive constants $R_1, R_2 \geq 1$ such that for all $i, j \in [n]$, we have

$$\frac{\|\nabla J_i(\theta_t)\|}{\|\nabla J_j(\theta_t)\|} \leq R_1, \quad \frac{\sqrt{\mathbb{V}(\pi_{\theta_t}(i))}}{\sqrt{\mathbb{V}(\pi_{\theta_t}(j))}} \leq R_2.$$

Assumption 5 bounds both the relative magnitudes of gradients and the relative reward variances across prompts, ensuring that the optimization dynamics remain balanced.

In the presence of weak cross-prompt interactions, we can still establish convergence guarantees for both GRPO and REINFORCE. The resulting bounds take a similar form to Theorem 3.1 and Theorem 3.2, but include additional scaling factors determined by constants M , R_1 , and R_2 in the relaxed assumptions. Their proofs are deferred to Appendix E.

Theorem 3.3. *Under Assumption 1 and Assumption 4, with step size $\eta = 1 / (\max(1, \frac{M}{2}) X_{\max}^2)$, the following descent inequality holds:*

$$\mathbb{E}[J_i(\theta_t)] - \mathbb{E}[J_i(\theta_{t-1})] \leq -\frac{\mathbb{E}[\|\nabla J_i(\theta_{t-1})\|^2]}{2n \max(1, \frac{M}{2}) X_{\max}^2}.$$

Consequently,

$$\sum_{t=0}^{T-1} \mathbb{E}[\|\nabla J_i(\theta_t)\|^2] \leq 2n \max(1, \frac{M}{2}) (1 - \pi_{\theta_0}^*(i)) X_{\max}^2,$$

Theorem 3.4. *Under Assumption 1 and Assumption 3–5, with step size $\eta = 1 / (2 \max(R_1, \frac{5M}{8}) R_2 X_{\max}^2)$, the following descent inequality holds:*

$$\mathbb{E}[J_i(\theta_t)] - \mathbb{E}[J_i(\theta_{t-1})] \leq -\frac{3\mathbb{E}[\|\nabla J_i(\theta_{t-1})\|^2]}{16n \max(R_1, \frac{5M}{8}) R_2 X_{\max}^2 C_{i_t}}.$$

Moreover,

$$\sum_{t=0}^{T-1} \mathbb{E}[\|\nabla J_i(\theta_t)\|^2] \leq 2n \max(R_1, \frac{5M}{8}) R_2 (1 - \pi_{\theta_0}^*(i)) X_{\max}^2 \cdot C(i, T),$$

$$\text{where } C(i, T) := \frac{8}{3T} \sum_{t=0}^{T-1} C_{i_t}.$$

Proof sketch. The proofs follow the same high-level structure as those of Theorems 3.1 and 3.2, but no longer rely on the exact orthogonality assumption in Assumption 2. Instead, the analysis leverages the relaxed cross-prompt interaction conditions in Assumptions 4 and 5.

Step 1: Decoupling across prompts. When the sampled prompt $i_t \neq l$, a second-order Taylor expansion of J_l around θ_t , together with Assumptions 4–5, shows that the update induced by q_{i_t} does not decrease J_l . That is, cross-prompt interference is non-negative and uniformly controlled

$$J_l(\theta_{t+1}) \geq J_l(\theta_t), \quad \text{for } i_t \neq l.$$

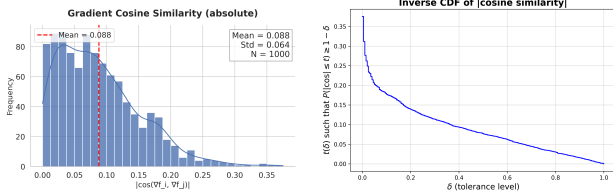
Step 2: One-step improvement for the active prompt.

When $i_t = l$, the argument proceeds analogously to the proofs of Theorems 3.1 and 3.2. Using the appropriate step size and the local smoothness bounds, one obtains a sufficient one-step improvement of J_l . Taking expectations over the random prompt selection and summing over iterations yields the stated convergence results. \square

4. Empirical Studies

4.1. Validation of the Orthogonal Assumption

Assumption 2 plays a central role in our theoretical analysis. It posits that representations associated with different



(a) Histogram of absolute cosine (b) Inverse CDF of absolute cosine similarity

Figure 1. Empirical validation of Assumption 2.

prompts are nearly orthogonal in the model’s representation space. Formally, for two distinct questions $i \neq j$, we expect the cosine similarity between their representations

$$\cos(v_i, v_j) := \frac{\langle v_i, v_j \rangle}{\|v_i\| \|v_j\|} \approx 0,$$

where v_i denotes the representation vector of question i . In our experiments, we take v_i to be the penultimate-layer hidden state of the language model.

We validate Assumption 2 on GSM8K (Cobbe et al., 2021) using Qwen2.5-MATH-1.5B (Yang et al., 2024). Specifically, we randomly sample 1,000 pairs of distinct questions, extract their penultimate-layer hidden states, pool these representations into sentence-level embeddings, and compute the absolute cosine similarity for each pair. As shown in Figure 1a, similarities are sharply concentrated near zero (mean ≈ 0.088 , std ≈ 0.064). Furthermore, the inverse CDF in Figure 1b indicates that over 90% of pairs exhibit absolute cosine similarity below 0.15, providing strong empirical support for the orthogonality assumption.

4.2. Validation of the Relaxed Assumption

First of all, a central assumption in our relaxed theoretical framework (Assumption 4) posits that cross-prompt gradient interactions remain bounded and constructive. Specifically, Assumption 4 requires the existence of a positive constant M such that for all distinct prompts $i, j \in [n]$:

$$M \langle \nabla J_i(\theta_t), \nabla J_j(\theta_t) \rangle \geq \frac{\|X_i \nabla J_j(\theta_t)\|^2}{\|X_i\|^2}.$$

Figure 2 shows the distribution of pairwise gradient cosine similarities. At initialization (Step 0), over 80% of pairs satisfy $|\cos| < 0.1$, indicating near-orthogonality where Assumption 4 holds trivially. During training, the distribution shifts slightly positive while remaining bounded ($M < 10$), confirming the assumption holds throughout optimization.

4.3. Validation of Local Curvature-Variance Connection

To empirically validate the local curvature-variance connection in Equation 7, we use the Fisher information matrix

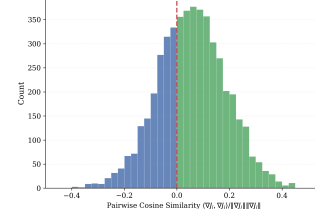


Figure 2. Empirical validation of Assumption 4

as a proxy for local curvature, following Liu et al. (2023). Given a mini-batch of prompts $\{q_i\}_{i=1}^B$ at iteration t , we proceed as follows: (i) we sample responses $\hat{o}_i \sim \pi_{\theta_t}(\cdot|q_i)$ for each prompt q_i ; (ii) we compute the mini-batch policy gradient $\nabla \hat{\mathcal{L}}_B(\theta_t) = \frac{1}{B} \sum_{i=1}^B \nabla \log \pi_{\theta_t}(\hat{o}_i|q_i)$; (iii) we estimate the diagonal Fisher Information using an efficient estimator $h(\theta_t) := \text{diag}(\hat{F}_{\text{eff}}(\theta_t)) := B \cdot \nabla \hat{\mathcal{L}}_B(\theta_t) \odot \nabla \hat{\mathcal{L}}_B(\theta_t)$, where \odot denotes element-wise multiplication. This estimator is unbiased in the sense that $\mathbb{E}_{\hat{o}}[h(\theta_t)] = \mathbb{E}_{\hat{o}}[\text{diag}(\hat{F}(\theta))]$. The resulting Fisher information $h(\theta_t)$ serves as our curvature proxy, capturing the local smoothness of the loss landscape. In Table 1, prompt-level Fisher entries exhibit a significant correlation with reward variance at the same iteration (mean Pearson ≈ 0.34 , $p < 0.01$), but show no meaningful correlation across different iterations. This suggests that the curvature–variance relationship holds locally rather than globally over training time.

Table 1. Temporal dependence between Fisher information and reward variance.

Time lag	Mean correlation	Significant
Same iter.	0.342	Yes ($p = 0.008$)
Different iter.	-0.028	No ($p = 0.18$)

4.4. Comparisons on LLM Reasoning Task

We conduct empirical evaluations to validate the effectiveness of variance normalization in GRPO and REINFORCE across tasks of varying difficulty.

Experimental setup. We use the Qwen2.5-Math-1.5B model as our base model and apply Low-Rank Adaptation (LoRA) for parameter-efficient fine-tuning. To study the effect of task difficulty and generalization, we employ two distinct benchmarks. First, we partition the GSM8K training set according to solution complexity into two subsets: *GSM8K-Easy* (4,695 examples) and *GSM8K-Hard* (1,909 examples). This partitioning is performed using Qwen2-7B-Instruct as an external evaluator, enabling a controlled analysis of the normalization scheme across varying difficulty regimes. Second, to assess the robustness of our results on broader mathematical domains, we incorporate the *MATH* benchmark (results see F.3), which consists

of competition-style problems spanning algebra, geometry, and number theory.

Normalization strategies. We compare normalization schemes within GRPO:

- GRPO (**standard**): $\hat{A}_{i,t} = \frac{r_i - \text{mean}(r)}{\text{std}(r)}$.
- No std normalization (**no_std**): $\hat{A}_{i,t} = r_i - \text{mean}(r)$.

Results and Discussion. We report the primary metric of sample accuracy, defined as the fraction of correct solutions among all generated responses. Figure 3 presents training accuracy on GSM8K Easy and Hard, with training phases identified via gradient orthogonality analysis (Section 4.1). The results reveal three distinct training regimes that closely align with our theoretical predictions.

Phase I: Near-Orthogonal regime (iterations 0–100). In the early training phase, prompt representations remain nearly orthogonal, as validated empirically in Section 4.1 (over 90% of gradient pairs satisfy $|\cos| < 0.1$). Despite this favorable geometric condition for Theorem 3.2, both normalization schemes exhibit comparable performance with overlapping trajectories. On GSM8K-Easy, both schemes improve from ≈ 0.45 to ≈ 0.70 with frequent crossings. On GSM8K-Hard, both follow similar trends, increasing from ≈ 0.20 to ≈ 0.40 . This observation can be attributed to the high reward variance characteristic of this regime. When accuracy lies in the range of 20–50%, the Bernoulli variance $\pi_\theta^*(i)(1 - \pi_\theta^*(i))$ approaches its maximum, leading to highly noisy gradient estimates. Such noise obscures the benefits of curvature-adaptive scaling, thereby diminishing the observable advantage of normalization during this phase.

Phase II: Low-variance transition (iterations 100–300). As training progresses, gradient orthogonality gradually degrades (Figure 4 in Appendix F, middle panel), yet the variance of pairwise gradient similarities remains low ($\text{std} \approx 0.066$). This regime is particularly favorable for GRPO’s normalization mechanism, under which *standard* establishes a clear and steadily widening advantage over *no_std*.

On GSM8K-Easy, *standard* reaches ≈ 0.95 while *no_std* attains ≈ 0.92 , opening a gap of nearly 3 percentage points. On GSM8K-Hard, the separation is more pronounced: *standard* climbs to ≈ 0.85 while *no_std* reaches only ≈ 0.78 , yielding a ~ 7 percentage point difference at iteration 300. The effectiveness of normalization in this phase can be explained as follows. Although strict orthogonality (Assumption 2) no longer holds, the low variance in cross-prompt gradient interactions ensures that the interference remains bounded, allowing the curvature-adaptive step size induced by normalization to operate effectively under the relaxed conditions of Theorem 3.4.

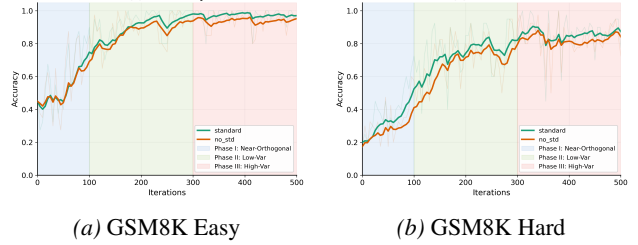


Figure 3. Training accuracy vs. iterations on GSM8K Easy (a) and Hard (b) with phase annotations. *standard* (green) uses variance normalization; *no_std* (orange) omits normalization. Shaded regions indicate three training regimes based on gradient geometry: **Phase I** (blue, 0–100): near-orthogonal regime where high reward variance leads to comparable performance despite favorable geometric conditions; **Phase II** (green, 100–300): low-variance regime where reduced orthogonality is offset by stable cross-prompt interactions, enabling *standard* to establish its advantage; **Phase III** (red, 300–500): high-variance regime where increased heterogeneity in gradient similarities limits further acceleration, though *standard* maintains its 2–3% lead. Curves are smoothed with exponential moving average ($\alpha = 0.18$).

Phase III: High-variance regime (iterations 300–500). In the late stage, cross-prompt gradient similarities exhibit substantially increased variance (std rises to ≈ 0.130 , Figure 4, right panel), indicating heterogeneous interference patterns across prompt pairs. Critically, *standard* maintains its advantage but the gap no longer widens. On GSM8K-Easy, both methods stabilize near 0.96–0.98, with *standard* having around 2 percentage point lead. On GSM8K-Hard, both methods fluctuate around 0.80–0.88, with *standard* maintaining about 3 percentage point advantage. The increased variance in gradient similarities limits the benefit of adaptive scaling. However, *standard* does not degrade relative to *no_std*. The advantage accumulated during Phase II is preserved throughout this regime. This suggests that GRPO’s normalization provides robust improvements overall, although its marginal gains diminish in the later stages of training as the model approaches saturation.

Role of gradient similarity variance. This analysis suggests that GRPO’s normalization is particularly valuable during the intermediate training phase when the Bernoulli reward variance $\pi_\theta^*(i)(1 - \pi_\theta^*(i))$ exits the regime near 0.25 and enters a moderate range. In this regime, reward variance serves as a reliable proxy for local curvature (Lemma 3.1), while sufficient heterogeneity across prompts is preserved to enable effective per-prompt adaptive scaling.

5. Conclusion

In this paper, we show that GRPO’s normalization can be viewed as a curvature-adaptive gradient mechanism: within-prompt reward variance estimates local smoothness of the policy gradient and rescales updates accordingly. This lens

clarifies when normalization helps, most notably when curvature varies across prompts or iterations and cross-prompt interference is controlled, and why GRPO can outperform REINFORCE beyond simple variance reduction. Theoretically, we prove faster convergence for GRPO under reasonable and mild assumptions. Empirically, experiments on GSM8K and MATH validate the curvature–variance connection and show that normalization improves stability and convergence, with the largest gains on harder, higher-variance prompts. Overall, our results provide a principled foundation for GRPO’s effectiveness and highlight adaptive scaling as a useful design principle for critic-free RL in LLM post-training.

References

Agarwal, A., Kakade, S. M., Lee, J. D., and Mahajan, G. On the theory of policy gradient methods: Optimality, approximation, and distribution shift. *Journal of Machine Learning Research*, 22(98):1–76, 2021.

Ahmadian, A., Cremer, C., Gallé, M., Fadaee, M., Kreutzer, J., Pietquin, O., Üstün, A., and Hooker, S. Back to basics: Revisiting reinforce style optimization for learning from human feedback in llms. *arXiv preprint arXiv:2402.14740*, 2024.

Bereket, M. and Leskovec, J. Uncalibrated reasoning: Grpo induces overconfidence for stochastic outcomes. *arXiv preprint arXiv:2508.11800*, 2025.

Chen, A., Li, A., Gong, B., Jiang, B., Fei, B., Yang, B., Shan, B., Yu, C., Wang, C., Zhu, C., et al. Minimax-m1: Scaling test-time compute efficiently with lightning attention. *arXiv preprint arXiv:2506.13585*, 2025.

Chu, X., Huang, H., Zhang, X., Wei, F., and Wang, Y. Gpg: A simple and strong reinforcement learning baseline for model reasoning. *arXiv preprint arXiv:2504.02546*, 2025.

Cobbe, K., Kosaraju, V., Bavarian, M., Chen, M., Jun, H., Kaiser, L., Plappert, M., Tworek, J., Hilton, J., Nakano, R., Hesse, C., and Schulman, J. Training verifiers to solve math word problems. *arXiv preprint arXiv:2110.14168*, 2021.

Gao, B., Song, F., Yang, Z., Cai, Z., Miao, Y., Dong, Q., Li, L., Ma, C., Chen, L., Xu, R., et al. Omni-math: A universal olympiad level mathematic benchmark for large language models. *arXiv preprint arXiv:2410.07985*, 2024.

Garrigos, G. and Gower, R. M. Handbook of convergence theorems for (stochastic) gradient methods. *arXiv preprint arXiv:2301.11235*, 2023.

Greensmith, E., Bartlett, P. L., and Baxter, J. Variance reduction techniques for gradient estimates in reinforcement learning. *Journal of Machine Learning Research*, 5(Nov): 1471–1530, 2004.

Guo, D., Yang, D., Zhang, H., Song, J., Zhang, R., Xu, R., Zhu, Q., Ma, S., Wang, P., Bi, X., et al. Deepseek-r1: Incentivizing reasoning capability in llms via reinforcement learning. *arXiv preprint arXiv:2501.12948*, 2025.

Hendrycks, D., Burns, C., Kadavath, S., Arora, A., Basart, S., Tang, E., Song, D., and Steinhardt, J. Measuring mathematical problem solving with the math dataset. *arXiv preprint arXiv:2103.03874*, 2021.

Hu, E. J., Shen, Y., Wallis, P., Allen-Zhu, Z., Li, Y., Wang, S., Wang, L., Chen, W., et al. Lora: Low-rank adaptation of large language models. *ICLR*, 1(2):3, 2022.

Hu, J., Zhang, Y., Han, Q., Jiang, D., Zhang, X., and Shum, H.-Y. Open-reasoner-zero: An open source approach to scaling up reinforcement learning on the base model. *arXiv preprint arXiv:2503.24290*, 2025.

Jain, S., Agrawal, A., and Goyal, N. Towards understanding the optimization landscape of grpo and its variants. In *First Workshop on Foundations of Reasoning in Language Models*, 2025.

Lambert, N. Reinforcement learning from human feedback. *arXiv preprint arXiv:2504.12501*, 2025.

Lambert, N., Morrison, J., Pyatkin, V., Huang, S., Ivison, H., Brahman, F., Miranda, L. J. V., Liu, A., Dziri, N., Lyu, S., et al. Tulu 3: Pushing frontiers in open language model post-training. *arXiv preprint arXiv:2411.15124*, 2024.

Li, Z., Xu, T., Zhang, Y., Lin, Z., Yu, Y., Sun, R., and Luo, Z.-Q. Remax: A simple, effective, and efficient reinforcement learning method for aligning large language models. *arXiv preprint arXiv:2310.10505*, 2023.

Lin, M. Q., Mei, J., Aghaei, M., Lu, M., Dai, B., Agarwal, A., Schuurmans, D., Szepesvari, C., and Vaswani, S. Rethinking the global convergence of softmax policy gradient with linear function approximation. *arXiv preprint arXiv:2505.03155*, 2025a.

Lin, Z., Lin, M., Xie, Y., and Ji, R. Cppo: Accelerating the training of group relative policy optimization-based reasoning models. *arXiv preprint arXiv:2503.22342*, 2025b.

Liu, H., Li, Z., Hall, D., Liang, P., and Ma, T. Sophia: A scalable stochastic second-order optimizer for language model pre-training. *arXiv preprint arXiv:2305.14342*, 2023.

Liu, Z., Chen, C., Li, W., Qi, P., Pang, T., Du, C., Lee, W. S., and Lin, M. Understanding r1-zero-like training: A critical perspective. *arXiv preprint arXiv:2503.20783*, 2025.

Mei, J., Xiao, C., Szepesvari, C., and Schuurmans, D. On the global convergence rates of softmax policy gradient methods. In *International conference on machine learning*, pp. 6820–6829. PMLR, 2020.

Mei, J., Zhong, Z., Dai, B., Agarwal, A., Szepesvari, C., and Schuurmans, D. Stochastic gradient succeeds for bandits. In *International Conference on Machine Learning*, pp. 24325–24360. PMLR, 2023.

Mroueh, Y., Dupuis, N., Belgodere, B., Nitsure, A., Rigotti, M., Greenwald, K., Navratil, J., Ross, J., and Rios, J. Revisiting group relative policy optimization: Insights into on-policy and off-policy training. *arXiv preprint arXiv:2505.22257*, 2025.

Ouyang, L., Wu, J., Jiang, X., Almeida, D., Wainwright, C., Mishkin, P., Zhang, C., Agarwal, S., Slama, K., Ray, A., et al. Training language models to follow instructions with human feedback. *Advances in neural information processing systems*, 35:27730–27744, 2022.

Pang, L. and Jin, R. On the theory and practice of grpo: A trajectory-corrected approach with fast convergence. *arXiv preprint arXiv:2508.02833*, 2025.

Rafailov, R., Sharma, A., Mitchell, E., Manning, C. D., Ermon, S., and Finn, C. Direct preference optimization: Your language model is secretly a reward model. *Advances in neural information processing systems*, 36: 53728–53741, 2023.

Schulman, J., Moritz, P., Levine, S., Jordan, M., and Abbeel, P. High-dimensional continuous control using generalized advantage estimation. *arXiv preprint arXiv:1506.02438*, 2015.

Schulman, J., Wolski, F., Dhariwal, P., Radford, A., and Klimov, O. Proximal policy optimization algorithms. *arXiv preprint arXiv:1707.06347*, 2017.

Shao, Z., Wang, P., Zhu, Q., Xu, R., Song, J., Bi, X., Zhang, H., Zhang, M., Li, Y., Wu, Y., et al. Deepseekmath: Pushing the limits of mathematical reasoning in open language models. *arXiv preprint arXiv:2402.03300*, 2024.

Simoni, M., Fontana, A., Rossolini, G., Saracino, A., and Mori, P. Gtpo: Stabilizing group relative policy optimization via gradient and entropy control. *arXiv preprint arXiv:2508.03772*, 2025.

Sutton, R. S., Barto, A. G., et al. *Reinforcement learning: An introduction*, volume 1. MIT press Cambridge, 1998.

Team, K., Du, A., Gao, B., Xing, B., Jiang, C., Chen, C., Li, C., Xiao, C., Du, C., Liao, C., et al. Kimi k1. 5: Scaling reinforcement learning with llms. *arXiv preprint arXiv:2501.12599*, 2025.

Vojnovic, M. and Yun, S.-Y. What is the alignment objective of grpo? *arXiv preprint arXiv:2502.18548*, 2025.

Wang, Y., Yang, Q., Zeng, Z., Ren, L., Liu, L., Peng, B., Cheng, H., He, X., Wang, K., Gao, J., et al. Reinforcement learning for reasoning in large language models with one training example. *arXiv preprint arXiv:2504.20571*, 2025.

Williams, R. J. Simple statistical gradient-following algorithms for connectionist reinforcement learning. *Machine learning*, 8(3):229–256, 1992.

Yang, A., Zhang, B., Hui, B., Gao, B., Yu, B., Li, C., Liu, D., Tu, J., Zhou, J., Lin, J., et al. Qwen2. 5-math technical report: Toward mathematical expert model via self-improvement. *arXiv preprint arXiv:2409.12122*, 2024.

Yu, Q., Zhang, Z., Zhu, R., Yuan, Y., Zuo, X., Yue, Y., Dai, W., Fan, T., Liu, G., Liu, L., et al. Dapo: An open-source llm reinforcement learning system at scale. *arXiv preprint arXiv:2503.14476*, 2025a.

Yu, Z., Peng, R., Ding, K., Li, Y., Peng, Z., Liu, M., Zhang, Y., Yuan, Z., Xin, H., Huang, W., et al. Formalmath: Benchmarking formal mathematical reasoning of large language models. *arXiv preprint arXiv:2505.02735*, 2025b.

Yuan, R., Du, S. S., Gower, R. M., Lazaric, A., and Xiao, L. Linear convergence of natural policy gradient methods with log-linear policies. *ArXiv*, abs/2210.01400, 2022. URL <https://api.semanticscholar.org/CorpusID:252693021>.

Zheng, C., Liu, S., Li, M., Chen, X.-H., Yu, B., Gao, C., Dang, K., Liu, Y., Men, R., Yang, A., et al. Group sequence policy optimization. *arXiv preprint arXiv:2507.18071*, 2025.

A. Table of Notation

Table 2. List of notations.

Notations	Definition
\mathcal{Q}	Set of questions / prompts
\mathcal{O}	Set of possible output sequences
$o^*(q)$	Unique correct output for prompt q (Assumption 1)
a_i	Index of the correct output for prompt q_i
r_i	Reward vector for prompt q_i
π_θ	Sequence-level policy of the LLM parameterized by θ
$\pi_\theta(i)$	Probability vector for prompt q_i under policy π_θ
$\pi_\theta^*(i)$	Success probability on prompt q_i under policy π_θ
$J_i(\theta)$	Objective function for prompt q_i under policy π_θ
$J(\theta)$	Global objective under policy π_θ
$J_{\text{GRPO}}(\theta)$	GRPO objective under policy π_θ
$x_{i,j}$	Feature vector for prompt-output pair (q_i, o_j)
X_i	Feature matrix for q_i with rows $x_{i,1}, \dots, x_{i,K}$
X_{\max}	Maximal feature norm, $X_{\max} = \max_{i \in [n]} \ X_i\ $
$H(\pi_\theta(i))$	Covariance matrix $\text{diag}(\pi_\theta(i)) - \pi_\theta(i)\pi_\theta(i)^\top$
$\text{Var}(\pi_\theta(i))$	Variance of reward for prompt q_i under policy π_θ
$\ \cdot\ $	Euclidean norm (vectors) / spectral norm (matrices)
$\text{diag}(v)$	Diagonal matrix with vector v on its diagonal
$\mathcal{B}(v, r)$	Euclidean ball $\{x \in \mathbb{R}^m : \ x - v\ _2 \leq r\}$
C_{i_t}	Prompt-wise variance bound introduced in Assumption 3
M	Cross-prompt gradient compatibility bound introduced in Assumption 4
R	Standard deviation lower bound introduced in Assumption 5

B. Gradient Update Rule of REINFORCE and GRPO

In this paper, we focus on the *log-linear policy parametrization* (Agarwal et al., 2021; Yuan et al., 2022). Specifically, we assume that for each question-output pair (q_i, o_j) , there exists a constant feature vector $x_{i,j} \in \mathbb{R}^d$ and the policy is given by:

$$\pi_\theta(o_j \mid q_i) := \frac{\exp(x_{i,j}^\top \theta)}{\sum_{l=1}^K \exp(x_{i,l}^\top \theta)}. \quad (9)$$

For ease of notation, we simply drop t from i_t whenever it clear in context. The update of Algorithm 1 takes the following form (Lin et al., 2025a):

$$\theta_t \leftarrow \theta_{t-1} + \eta X_i^\top \left(\text{diag}(\pi_{\theta_{t-1}}(i)) - \pi_{\theta_{t-1}}(i)\pi_{\theta_{t-1}}^\top(i) \right) r_i. \quad (10)$$

Under Assumption 1, the update of REINFORCE (Algorithm 1) can be simplified as:

$$\theta_t \leftarrow \theta_{t-1} + \eta \left(\pi_{\theta_{t-1}}^*(i) (1 - \pi_{\theta_{t-1}}^*(i)x_{i,a_i} - \pi_{\theta_{t-1}}^*(i) \sum_{j \neq a_i} [\pi_{\theta_{t-1}}(i)]_j \cdot x_{i,j}) \right). \quad (11)$$

Similarly, the update of GRPO (Algorithm 2) can be simplified as:

$$\theta_t \leftarrow \theta_{t-1} + \eta \left(\sqrt{\pi_{\theta_{t-1}}^*(i)(1 - \pi_{\theta_{t-1}}^*(i))} x_{i,a_i} - \sqrt{\frac{\pi_{\theta_{t-1}}^*(i)}{1 - \pi_{\theta_{t-1}}^*(i)}} \sum_{j \neq a_i} [\pi_{\theta_{t-1}}(i)]_j \cdot x_{i,j} \right). \quad (12)$$

C. Analysis of the Local Smoothness Constant

C.1. Proof of Lemma 3.1

According to Lemma 17 in (Lin et al., 2025a), for any $y \in \mathbb{R}^d$, we have

$$y^\top \nabla^2 J_i(\theta) y = (H(\pi_\theta(i)) r_i)^\top (X_i y \odot X_i y) - 2 (H(\pi_\theta(i)) r_i)^\top (X_i y) (\pi_\theta^\top(i) X_i y)$$

where $H(\pi_\theta(i))$ is defined as $H(\pi_\theta) := \text{diag}(\pi_\theta(i)) - \pi_\theta(i) \pi_\theta^\top(i) \in \mathbb{R}^{K \times K}$ and \odot denotes the Hadamard (component-wise) product. Using the triangle inequality and Cauchy-Schwarz inequality, we get

$$\begin{aligned} |y^\top \nabla^2 J_i(\theta) y| &\leq |(H(\pi_\theta(i)) r_i)^\top (X_i y \odot X_i y)| + 2 |(H(\pi_\theta(i)) r_i)^\top (X_i y)| \cdot |(\pi_\theta^\top(i) X_i y)| \\ &\leq \|(H(\pi_\theta(i)) r_i)\|_\infty \|X_i y \odot X_i y\|_1 + 2 \|H(\pi_\theta(i)) r_i\| \cdot \|X_i y\| \cdot \|\pi_\theta(i)\| \cdot \|X_i y\| \\ &= \|(H(\pi_\theta(i)) r_i)\|_\infty \|X_i y\|^2 + 2 \|H(\pi_\theta(i)) r_i\| \cdot \|\pi_\theta(i)\| \cdot \|X_i y\|^2 \\ &\leq \|(H(\pi_\theta(i)) r_i)\|_\infty \|X_i y\|^2 + 2 \|H(\pi_\theta(i)) r_i\| \cdot \|X_i y\|^2. \end{aligned} \quad (13)$$

The last inequality follows because $\|\pi_\theta(i)\| \leq \|\pi_\theta(i)\|_1 = 1$. According to Assumption 1, we have

$$[H(\pi_\theta(i)) r_i]_j = \begin{cases} \pi_\theta^*(i)(1 - \pi_\theta^*(i)), & \text{if } j = a_i \\ -\pi_\theta^*(i)[\pi_\theta(i)]_j, & \text{if } j \neq a_i \end{cases}$$

With this expression, we get

$$\|H(\pi_\theta(i)) r_i\|_\infty = \pi_\theta^*(i)(1 - \pi_\theta^*(i)), \quad (14)$$

and

$$\begin{aligned} \|H(\pi_\theta(i)) r_i\| &= \pi_\theta^*(i) \sqrt{(1 - \pi_\theta^*(i))^2 + \sum_{j \neq a_i} [\pi_\theta(i)]_j^2} \\ &\leq \pi_\theta^*(i) \sqrt{(1 - \pi_\theta^*(i))^2 + \sum_{j \neq a_i} [\pi_\theta(i)]_j (1 - \pi_\theta^*(i))} \\ &= \sqrt{2} \pi_\theta^*(i)(1 - \pi_\theta^*(i)). \end{aligned} \quad (15)$$

Combining (14) and (15) with (13), we get

$$\begin{aligned} |y^\top \nabla^2 J_i(\theta) y| &\leq \|(H(\pi_\theta(i)) r_i)\|_\infty \|X_i y\|^2 + 2 \|H(\pi_\theta(i)) r_i\| \cdot \|X_i y\|^2 \\ &\leq (2\sqrt{2} + 1) \pi_\theta^*(i)(1 - \pi_\theta^*(i)) \|X_i y\|^2 \\ &\leq (2\sqrt{2} + 1) \pi_\theta^*(i)(1 - \pi_\theta^*(i)) \|X_i\|^2 \|y\|^2 \\ &\leq 4 \pi_\theta^*(i)(1 - \pi_\theta^*(i)) X_{\max}^2 \|y\|^2 \end{aligned} \quad (16)$$

where the third inequality is due to the definition of operator norm, and the last inequality is by definition of X_{\max} . Note that

$$\|\nabla^2 J_i(\theta)\| = \max_y \frac{|y^\top \nabla^2 J_i(\theta) y|}{\|y\|^2}$$

for symmetric Hessian matrix $\nabla^2 J_i(\theta)$, which completes the proof.

C.2. Proof of Lemma 3.2

According to (11), the gradient of $J_i(\theta)$ takes the following form:

$$\nabla J_i(\theta) = x_{a_i}^\top (1 - \pi_{\theta_t}^*(i)) \pi_{\theta_t}^*(i) - \sum_{j \neq a_i} x_j^\top \pi_{\theta_t}(i)_j \cdot \pi_{\theta_t}^*(i).$$

Note that a matrix's operator norm is larger than the norm of any of its row vector, we get

$$\begin{aligned}
 \|\nabla J_i(\theta)\| &\leq \|x_{a_i}\|(1 - \pi_{\theta_t}^*(i))\pi_{\theta_t}^*(i) + \sum_{j \neq a_i} \|x_j\|\pi_{\theta_t}(i)_j \cdot \pi_{\theta_t}^*(i) \\
 &\leq \|X_i\|(1 - \pi_{\theta_t}^*(i))\pi_{\theta_t}^*(i) + \sum_{j \neq a_i} \|X_i\|\pi_{\theta_t}(i)_j \cdot \pi_{\theta_t}^*(i) \\
 &= 2\|X_i\|(1 - \pi_{\theta_t}^*(i))\pi_{\theta_t}^*(i) \\
 &\leq \frac{1}{2}X_{\max}
 \end{aligned}$$

where the last inequality is due to the definition of X_{\max} , finishing the proof.

C.3. Proof of Lemma 3.3

By Assumption 1, the objective $J_i(\theta)$ is same as $\pi_{\theta}^*(i)$. From Lemma 3.2, $J_i(\theta)$ is $\frac{1}{2}X_{\max}$ -Lipschitz. Consequently, for any $\theta' \in \mathcal{B}\left(\theta, \frac{1}{X_{\max}}\sqrt{\pi_{\theta}^*(i)(1 - \pi_{\theta}^*(i))}\right)$, we have

$$|\pi_{\theta'}^*(i) - \pi_{\theta}^*(i)| \leq \frac{1}{2}X_{\max} \cdot \frac{1}{X_{\max}} \cdot \sqrt{\pi_{\theta}^*(i)(1 - \pi_{\theta}^*(i))} = \frac{1}{2}\sqrt{\pi_{\theta}^*(i)(1 - \pi_{\theta}^*(i))}.$$

Combining with Lemma 3.1,

$$\|\nabla^2 J_i(\theta')\| \leq \max_l 4X_{\max}^2 \cdot l(1 - l)$$

over $\mathcal{B}\left(\theta, \frac{1}{X_{\max}}\sqrt{\pi_{\theta}^*(i)(1 - \pi_{\theta}^*(i))}\right)$, where l satisfies

$$|l - \pi_{\theta}^*(i)| \leq \frac{1}{2}\sqrt{\pi_{\theta}^*(i)(1 - \pi_{\theta}^*(i))}.$$

We denote $\pi_{\theta}^*(i)$ as a . Thus, proving Lemma 3.3 is equivalent as proving

$$f(a) := \max_{l \in [a - \frac{\sqrt{a(1-a)}}{2}, a + \frac{\sqrt{a(1-a)}}{2}]} \frac{4l(1-l)}{\sqrt{a(1-a)}} \leq \frac{5}{2}.$$

WLOG, we assume $a \in [0, \frac{1}{2}]$ and consider two cases.

Case 1: When $a \in [\frac{1}{2} - \frac{\sqrt{5}}{10}, \frac{1}{2}]$, we know that

$$\frac{1}{2} \in [a - \frac{\sqrt{a(1-a)}}{2}, a + \frac{\sqrt{a(1-a)}}{2}],$$

which implies that

$$f(a) = \frac{1}{\sqrt{a(1-a)}} \leq f(\frac{1}{2} - \frac{\sqrt{5}}{10}) = \sqrt{5} \leq \frac{5}{2}.$$

Case 2: When $a \in [0, \frac{1}{2} - \frac{\sqrt{5}}{10}]$, we know that

$$\frac{1}{2} \notin [a - \frac{\sqrt{a(1-a)}}{2}, a + \frac{\sqrt{a(1-a)}}{2}].$$

Because $g(l) = l(1 - l)$ is monotonically increasing in $[0, \frac{1}{2}]$, we can obtain

$$f(a) = \frac{4(a + \frac{\sqrt{a(1-a)}}{2})(1 - a - \frac{\sqrt{a(1-a)}}{2})}{\sqrt{a(1-a)}} = 3\sqrt{a(1-a)} + (2 - 4a).$$

$f(a)$ takes its maximum when $a = \frac{1}{10}$ and $f(a) = \frac{5}{2}$.

Combining the above two cases, we conclude the lemma.

D. Convergence Analysis under Orthogonal Representation Assumption

D.1. Auxiliary Lemma

Lemma D.1. *Under Assumption 1 and 2, for any $i, j \in [n], i \neq j$ and $\theta \in \mathbb{R}^d$, we have*

$$\nabla J_i(\theta)^\top \nabla J_j(\theta) = 0 \quad (17)$$

Proof. According to (10), we get

$$\begin{aligned} \nabla J_i(\theta)^\top \nabla J_j(\theta) &= r_i^\top (\text{diag}(\pi_\theta(i)) - \pi_\theta(i)\pi_\theta^\top(i)) X_i X_j^\top (\text{diag}(\pi_\theta(j)) - \pi_\theta(j)\pi_\theta^\top(j)) r_j \\ &= r_i^\top (\text{diag}(\pi_\theta(i)) - \pi_\theta(i)\pi_\theta^\top(i)) 0 (\text{diag}(\pi_\theta(j)) - \pi_\theta(j)\pi_\theta^\top(j)) r_j \\ &= 0, \end{aligned}$$

where the second step is by Assumption 2. \square

D.2. Proof of Theorem 3.1

We consider a specific question q_l . Combining Lemma D.1 with *log-linear policy parameterization* in our setting, if question q_{i_t} is selected on iteration t in Algorithm 1, we get

$$\begin{aligned} J_j(\theta_t) &= J_j(\theta_{t-1} + \eta \nabla J_i(\theta_{t-1})) \\ &= J_j(\theta_{t-1}) \end{aligned} \quad (18)$$

for any $i_t \neq l$. That is, the parameter update on question q_{i_t} will not affect the expected reward on other questions.

If question $i_t = l$ is selected on iteration t in Algorithm 1, we have

$$\begin{aligned} J_l(\theta_t) - J_l(\theta_{t-1}) &\geq \langle \theta_t - \theta_{t-1}, \nabla J_l(\theta_{t-1}) \rangle - \frac{X_{\max}^2}{2} \|\theta_t - \theta_{t-1}\|^2 \\ &= (\eta - \frac{X_{\max}^2}{2} \eta^2) \|\nabla J_l(\theta_{t-1})\|^2 \\ &= \frac{1}{2X_{\max}^2} \|\nabla J_l(\theta_{t-1})\|^2 \end{aligned} \quad (19)$$

where the first step is by ??, which also indicate that $J_i(\theta)$ is X_{\max}^2 -weakly convex. Combining (18) and (19) and taking the expectation over i_t , we get

$$\mathbb{E}[J_l(\theta_t)] - \mathbb{E}[J_l(\theta_{t-1})] \geq \frac{1}{2nX_{\max}^2} \|\nabla J_l(\theta_{t-1})\|^2. \quad (20)$$

Summing up (20) for $t = 1, \dots, T$, we have

$$\frac{1}{2nX_{\max}^2} \sum_{t=0}^{T-1} \mathbb{E}[\|\nabla J_l(\theta_{t-1})\|^2] \leq \mathbb{E}[J_l(\theta_T)] - J_l(\theta_0) \leq 1 - \pi_{\theta_0}^*(l).$$

This directly leads to

$$\min_{t \in \{0, 1, \dots, T-1\}} \mathbb{E}[\|\nabla J_l(\theta_t)\|^2] \leq \frac{2n(1 - \pi_{\theta_0}^*(l))X_{\max}^2}{T}.$$

D.3. Proof of Theorem 3.2

Similar to (18) in the proof of Theorem 3.1, the gradient update based on question q_i does not affect the objective for question q_l if $i \neq l$. That is,

$$J_l(\theta_t) = \begin{cases} J_l(\theta_{t-1}), & \text{if } i_t \neq l \\ J_l(\theta_t), & \text{if } i_t = l. \end{cases} \quad (21)$$

Consider the case where $i_t = l$, from the parameter update rule in Algorithm 2, we get

$$\theta_t = \theta_{t-1} + \eta \left(\sqrt{\pi_{\theta_{t-1}}^*(l)(1 - \pi_{\theta_{t-1}}^*(l))} x_{l,a_l} - \sqrt{\frac{\pi_{\theta_{t-1}}^*(l)}{1 - \pi_{\theta_{t-1}}^*(l)}} \sum_{j \neq a_l} [\pi_{\theta_{t-1}}(l)]_j \cdot x_{l,j} \right).$$

Also, by setting $\eta = \frac{1}{2X_{\max}^2}$, we have

$$\begin{aligned} & \|\eta \left(\sqrt{\pi_{\theta_{t-1}}^*(l)(1 - \pi_{\theta_{t-1}}^*(l))} x_{l,a_l} - \sqrt{\frac{\pi_{\theta_{t-1}}^*(l)}{1 - \pi_{\theta_{t-1}}^*(l)}} \sum_{j \neq a_l} [\pi_{\theta_{t-1}}(l)]_j \cdot x_{l,j} \right)\| \\ &= \frac{1}{2X_{\max}^2} \left\| \left(\sqrt{\pi_{\theta_{t-1}}^*(l)(1 - \pi_{\theta_{t-1}}^*(l))} x_{l,a_l} - \sqrt{\frac{\pi_{\theta_{t-1}}^*(l)}{1 - \pi_{\theta_{t-1}}^*(l)}} \sum_{j \neq a_l} [\pi_{\theta_{t-1}}(l)]_j \cdot x_{l,j} \right) \right\| \\ &\leq \frac{1}{2X_{\max}^2} \left(\sqrt{\pi_{\theta_{t-1}}^*(l)(1 - \pi_{\theta_{t-1}}^*(l))} \|x_{l,a_l}\| + \sqrt{\frac{\pi_{\theta_{t-1}}^*(l)}{1 - \pi_{\theta_{t-1}}^*(l)}} \sum_{j \neq a_l} [\pi_{\theta_{t-1}}(l)]_j \cdot \|x_{l,j}\| \right) \\ &\leq \frac{1}{2X_{\max}^2} (2\sqrt{\pi_{\theta_{t-1}}^*(l)(1 - \pi_{\theta_{t-1}}^*(l))} X_{\max}) \\ &= \frac{1}{X_{\max}} \cdot \sqrt{\pi_{\theta_{t-1}}^*(l)(1 - \pi_{\theta_{t-1}}^*(l))}. \end{aligned}$$

This implies that $\theta_t \in \mathcal{B}(\theta, \frac{1}{X_{\max}} \cdot \sqrt{\pi_{\theta_{t-1}}^*(l)(1 - \pi_{\theta_{t-1}}^*(l))})$. According to Lemma 3.3, we could obtain

$$\begin{aligned} J_l(\theta_t) &\geq J_l(\theta_{t-1}) + \langle \theta_t - \theta_{t-1}, \nabla J_l(\theta_{t-1}) \rangle - \frac{5}{4} X_{\max}^2 \cdot \sqrt{\pi_{\theta_{t-1}}^*(l)(1 - \pi_{\theta_{t-1}}^*(l))} \|\theta_t - \theta_{t-1}\|^2 \\ &= J_l(\theta_{t-1}) + \frac{3}{16X_{\max}^2 \sqrt{\pi_{\theta_{t-1}}^*(l)(1 - \pi_{\theta_{t-1}}^*(l))}} \|\nabla J_l(\theta_{t-1})\|^2 \\ &\geq J_l(\theta_{t-1}) + \frac{3}{16X_{\max}^2 C_{l_{t-1}}} \|\nabla J_l(\theta_{t-1})\|^2 \end{aligned} \tag{22}$$

where the last step is by Assumption 3. Combining (21) and (22) and taking the expectation over i_t , we obtain

$$\mathbb{E}[J_l(\theta_t)] \geq \mathbb{E}[J_l(\theta_{t-1})] + \frac{3}{16nX_{\max}^2 C_{l_{t-1}}} \mathbb{E}[\|\nabla J(\theta_{t-1})\|^2]. \tag{23}$$

Summing up (23) for $t = 1, \dots, T$, we get

$$\mathbb{E}[J_l(\theta_T)] \geq J_l(\theta_0) + \sum_{t=0}^{T-1} \frac{3}{16nX_{\max}^2 C_{l_t}} \mathbb{E}[\|\nabla J(\theta_{t-1})\|^2]. \tag{24}$$

According to the Cauchy-Schwarz inequality, we have

$$\min_{t \in \{0, 1, \dots, T-1\}} \mathbb{E}[\|\nabla J_l(\theta_t)\|^2] \leq \frac{2n(1 - \pi_{\theta_0}^*(l))X_{\max}^2}{T} \frac{8 \sum_{t=0}^{T-1} C_{l_t}}{3T}.$$

E. Convergence Analysis under Relaxed Assumptions

E.1. Proof of Theorem 3.3

Following the proof of Theorem 3.1 in Section D.2, for a fixed question q_l , we analyze the update at timestep t by distinguishing between the two cases $i_t \neq l$ and $i_t = l$.

If question $i_t = l$ is selected at iteration t in Algorithm 1, then

$$\begin{aligned}
 J_l(\theta_t) - J_l(\theta_{t-1}) &\geq \langle \theta_t - \theta_{t-1}, \nabla J_l(\theta_{t-1}) \rangle - \frac{X_{\max}^2}{2} \|\theta_t - \theta_{t-1}\|^2 \\
 &= (\eta - \frac{X_{\max}^2}{2} \eta^2) \|\nabla J_l(\theta_{t-1})\|^2 \\
 &\geq \frac{1}{2 \max(1, \frac{M}{2}) X_{\max}^2} \|\nabla J_l(\theta_{t-1})\|^2
 \end{aligned} \tag{25}$$

with the same argument as in (19).

If question $i_t \neq l$ is selected at iteration t in Algorithm 1, applying Taylor expansion, we get

$$J_l(\theta_t) - J_l(\theta_{t-1}) = \langle \theta_t - \theta_{t-1}, \nabla J_l(\theta_{t-1}) \rangle + \frac{1}{2} \eta^2 \left(\nabla J_{i_t}(\theta_{t-1}) \right)^\top \nabla^2 J_l(\theta') \left(\nabla J_{i_t}(\theta_{t-1}) \right) \tag{26}$$

for some $\theta' \in \mathbb{R}^d$. According to Lemma 17 in (Lin et al., 2025a) and (10), we have

$$\begin{aligned}
 J_l(\theta_t) - J_l(\theta_{t-1}) &= \eta \langle \nabla J_l(\theta_{t-1}), \nabla J_{i_t}(\theta_{t-1}) \rangle \\
 &\quad + \frac{1}{2} \eta^2 (H(\pi_{\theta'}(l)) r_l)^\top (X_l \nabla J_{i_t}(\theta_{t-1}) \odot X_l \nabla J_{i_t}(\theta_{t-1})) \\
 &\quad + \eta^2 (H(\pi_{\theta'}(l)) r_l)^\top (X_l \nabla J_{i_t}(\theta_{t-1})) (\pi_{\theta'}(l)^\top X_l \nabla J_{i_t}(\theta_{t-1})) \\
 &\geq \eta \langle \nabla J_l(\theta_t), \nabla J_{i_t}(\theta_t) \rangle - 2\eta^2 \pi_{\theta'}^*(l) (1 - \pi_{\theta'}^*(l)) \|X_l \nabla J_{i_t}(\theta_{t-1})\|^2 \\
 &\geq \eta \langle \nabla J_l(\theta_t), \nabla J_{i_t}(\theta_t) \rangle - \frac{\eta^2}{2} \|X_l \nabla J_{i_t}(\theta_{t-1})\|^2 \\
 &\geq \frac{\eta \|X_l \nabla J_{i_t}(\theta_{t-1})\|^2}{M \|X_l\|^2} - \frac{\eta^2}{2} \|X_l \nabla J_{i_t}(\theta_{t-1})\|^2 \\
 &\geq 0,
 \end{aligned} \tag{27}$$

where the second inequality is due to (16) and the fourth inequality is because Assumption 4. Combining (25) and (27) and taking the expectation over i_t , we get

$$\mathbb{E}[J_l(\theta_t)] - \mathbb{E}[J_l(\theta_{t-1})] \geq \frac{1}{2 \max(1, \frac{M}{2}) n X_{\max}^2} \|\nabla J_l(\theta_{t-1})\|^2. \tag{28}$$

Summing up (28) for $t = 1, \dots, T$, we get

$$\frac{1}{2n \max(1, \frac{M}{2}) X_{\max}^2} \sum_{t=0}^{T-1} \mathbb{E}[\|J_l(\theta_{t-1})\|^2] \leq \mathbb{E}[J_l(\theta_T)] - J_l(\theta_0) \leq 1 - \pi_{\theta_0}^*(l).$$

This directly leads to

$$\min_{t \in \{0, 1, \dots, T-1\}} \mathbb{E}[\|\nabla J_l(\theta_t)\|^2] \leq \frac{2n \max(1, \frac{M}{2}) (1 - \pi_{\theta_0}^*(l)) X_{\max}^2}{T}.$$

E.2. Proof of Theorem 3.4

Following the proof of Theorem 3.1 in Section D.2, for a fixed question q_l , we analyze the update at timestep t by distinguishing between the two cases $i_t \neq l$ and $i_t = l$.

If question $i_t = l$ is selected at iteration t in Algorithm 2, then

$$\begin{aligned}
 J_l(\theta_t) &\geq J_l(\theta_{t-1}) + \langle \theta_t - \theta_{t-1}, \nabla J_l(\theta_{t-1}) \rangle - \frac{5}{4} X_{\max}^2 \cdot \sqrt{\pi_{\theta_{t-1}}^*(l) (1 - \pi_{\theta_{t-1}}^*(l))} \|\theta_t - \theta_{t-1}\|^2 \\
 &= J_l(\theta_{t-1}) + \frac{3}{16 \max(R_1, \frac{5M}{8}) R_2 X_{\max}^2 \sqrt{\pi_{\theta}^*(l) (1 - \pi_{\theta}^*(l))}} \|\nabla J_l(\theta_{t-1})\|^2 \\
 &\geq J_l(\theta_{t-1}) + \frac{3}{16 \max(R_1, \frac{5M}{8}) R_2 X_{\max}^2 C_{l_{t-1}}} \|\nabla J_l(\theta_{t-1})\|^2
 \end{aligned} \tag{29}$$

with the same argument as in (22).

If question $i_t \neq l$ is selected at iteration t in Algorithm 2, applying Taylor expansion, we get

$$\begin{aligned} J_l(\theta_t) - J_l(\theta_{t-1}) &= \frac{\eta}{\sqrt{\mathbb{V}(\pi_{\theta_{t-1}}(i_t))}} \langle \theta_t - \theta_{t-1}, \nabla J_l(\theta_{t-1}) \rangle \\ &+ \frac{\eta^2}{2\mathbb{V}(\pi_{\theta_{t-1}}(i_t))} \left(\nabla J_{i_t}(\theta_{t-1}) \right)^\top \nabla^2 J_l(\theta') \left(\nabla J_{i_t}(\theta_{t-1}) \right) \end{aligned} \quad (30)$$

for some $\theta' \in \mathbb{R}^d$. According to Lemma 17 in Lin et al. (2025a) and (10), we have

$$\begin{aligned} J_l(\theta_t) - J_l(\theta_{t-1}) &= \frac{\eta}{\sqrt{\mathbb{V}(\pi_{\theta_{t-1}}(i_t))}} \langle \nabla J_l(\theta_{t-1}), \nabla J_{i_t}(\theta_{t-1}) \rangle \\ &+ \frac{\eta^2}{2\mathbb{V}(\pi_{\theta_{t-1}}(i_t))} (H(\pi_{\theta'}(l))r_l)^\top (X_l \nabla J_{i_t}(\theta_{t-1}) \odot X_l \nabla J_{i_t}(\theta_{t-1})) \\ &+ \frac{\eta^2}{\mathbb{V}(\pi_{\theta_{t-1}}(i_t))} (H(\pi_{\theta'}(l))r_l)^\top (X_l \nabla J_{i_t}(\theta_{t-1})) (\pi_{\theta'}(l)^\top X_l \nabla J_{i_t}(\theta_{t-1})) \\ &\geq \frac{\eta}{\sqrt{\mathbb{V}(\pi_{\theta_{t-1}}(i_t))}} \langle \nabla J_l(\theta_t), \nabla J_{i_t}(\theta_t) \rangle - \frac{5\sqrt{\mathbb{V}(\pi_{\theta_{t-1}}(l))}\eta^2}{4\mathbb{V}(\pi_{\theta_{t-1}}(i_t))} \|X_l \nabla J_{i_t}(\theta_{t-1})\|^2 \\ &\geq \frac{\eta \|X_l \nabla J_{i_t}(\theta_{t-1})\|^2}{M \cdot \sqrt{\mathbb{V}(\pi_{\theta_{t-1}}(i_t))} \|X_l\|^2} - \frac{5\sqrt{\mathbb{V}(\pi_{\theta_{t-1}}(l))}\eta^2}{4\mathbb{V}(\pi_{\theta_{t-1}}(i_t))} \|X_l \nabla J_{i_t}(\theta_{t-1})\|^2 \\ &\geq 0, \end{aligned} \quad (31)$$

where the second inequality is due to Lemma 3.3 and the third inequality is because Assumption 4 and Assumption 5.

Combining (29) and (31) and taking the expectation over i_t , we obtain

$$\mathbb{E}[J_l(\theta_t)] \geq \mathbb{E}[J_l(\theta_{t-1})] + \frac{3}{16n \max(R_1 R_2, \frac{M}{2}) X_{\max}^2 C_{l_{t-1}}} \mathbb{E}[\|\nabla J(\theta_{t-1})\|^2]. \quad (32)$$

Summing up (32) for $t = 1, \dots, T$, we get

$$\mathbb{E}[J_l(\theta_T)] \geq J_l(\theta_0) + \sum_{t=0}^{T-1} \frac{3}{16n \max(R_1 R_2, \frac{M}{2}) X_{\max}^2 C_{l_t}} \mathbb{E}[\|\nabla J(\theta_{t-1})\|^2]. \quad (33)$$

According to the Cauchy-Schwarz inequality, we have

$$\min_{t \in \{0, 1, \dots, T-1\}} \mathbb{E}[\|\nabla J_l(\theta_t)\|^2] \leq \frac{2n \max(R_1 R_2, \frac{M}{2})(1 - \pi_{\theta_0}^*(l)) X_{\max}^2}{T} \frac{8 \sum_{t=0}^{T-1} C_{l_t}}{3T}.$$

F. Additional Experimental Results

F.1. Evolution of Gradient Orthogonality During Training

To complement the validation of Assumption 2 (orthogonal representation) in Section 4.1, we examine how cross-prompt gradient interactions evolve throughout the training process. This analysis provides empirical support for both the exact orthogonality assumption (Assumption 2) and the relaxed assumption (Assumption 4).

Experimental Setup. We track pairwise gradient cosine similarities across 100 randomly sampled questions from GSM8K, yielding $\binom{100}{2} = 4,950$ gradient pairs per checkpoint. For each pair of distinct prompts $i \neq j$, we compute

$$\cos(\nabla J_i(\theta_t), \nabla J_j(\theta_t)) = \frac{\langle \nabla J_i(\theta_t), \nabla J_j(\theta_t) \rangle}{\|\nabla J_i(\theta_t)\| \|\nabla J_j(\theta_t)\|}.$$

We analyze the distribution at three representative checkpoints: Step 0 (initialization), Step 260 (mid-training), and Step 500 (convergence).

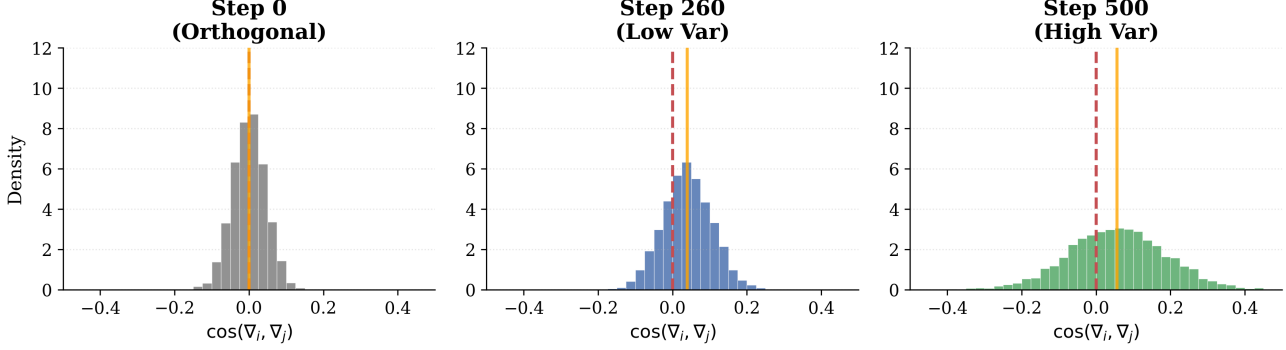


Figure 4. Evolution of Pairwise Gradient Cosine Similarity During GRPO Training on GSM8K. Distribution of cosine similarities between per-prompt gradient pairs across 100 questions (4,950 pairs) at three training stages. The red dashed line indicates $\cos = 0$ (orthogonality), and the orange solid line indicates the mean. (Left) Step 0: Near-perfect orthogonality with over 90% of pairs satisfying $|\cos| < 0.1$. (Middle) Step 260: Gradients begin developing positive correlations while maintaining low variance ($\text{std} = 0.066$). (Right) Step 500: Increased variance ($\text{std} = 0.130$) with the distribution spreading while remaining centered near zero.

Results. Figure 4 illustrates the evolution of gradient cosine similarity distributions across training. We observe three distinct phases:

Phase I: Orthogonal Regime (Step 0). At initialization, gradient directions are nearly orthogonal, consistent with the theoretical expectation for high-dimensional random vectors. Specifically, over 80% of pairs satisfy $|\cos| < 0.1$, with mean ≈ 0 and standard deviation ≈ 0.045 . This confirms that Assumption 2 holds approximately at initialization, and Assumption 4 is trivially satisfied since both sides of the inequality approach zero when gradients are orthogonal.

Phase II: Low-Variance Transition (Step 260). As training progresses, gradients develop weak positive correlations (mean ≈ 0.04 , with 72.7% positive pairs), indicating that prompts begin sharing beneficial update directions. The variance remains low ($\text{std} \approx 0.066$), suggesting that the model learns generalizable features without significant gradient interference. The bounded M value confirms that Assumption 4 continues to hold.

Phase III: High-Variance Regime (Step 500). The distribution spreads further ($\text{std} \approx 0.130$) while maintaining a weakly positive mean (≈ 0.056). The increased variance reflects the heterogeneous nature of mathematical reasoning tasks, some prompt pairs benefit from similar updates while others require distinct optimization directions. Despite this spread, the M bound remains finite ($M \approx 418 < 500$ for $n = 100$ prompts), confirming that Assumption 4 is satisfied throughout training.

Implications. These observations align with our theoretical framework in several ways:

- The gradual shift from orthogonality to weak positive correlation indicates that GRPO learns shared representations across prompts without catastrophic interference.
- The bounded M value throughout training validates the applicability of our relaxed theoretical framework (Theorem 3.4) to practical GRPO optimization.
- The three-phase pattern explains the training dynamics observed in Figure 4: GRPO achieves maximum acceleration in Phase I when orthogonality is strongest, maintains advantage in Phase II as variance decreases, and the gap stabilizes in Phase III as cross-prompt interference increases.

F.2. Quantitative Summary

Table 3 summarizes the key statistics across training phases, providing quantitative support for the assumptions in our theoretical analysis.

F.3. Additional Results on MATH Benchmark

To assess the generalization of our findings beyond grade-school arithmetic, we further evaluate the normalization strategies on the **MATH** benchmark (Level 2 subset), which involves more diverse and complex reasoning tasks (e.g., Algebra, Geometry).

Table 3. Statistics of pairwise gradient cosine similarities at different training stages (GSM8K, $n = 100$ questions, 4,950 pairs).

Stage	Mean	Std	$\cos > 0$	$ \cos < 0.1$	M Bound	Assumption
Step 0 (Orthogonal)	0.000	0.045	50.5%	97.7%	89	Asm. 2 holds
Step 260 (Low Var)	0.039	0.066	72.7%	80.3%	250	Asm. 4 holds
Step 500 (High Var)	0.056	0.130	66.4%	52.4%	418	Asm. 4 holds

As shown in Figure 5, the training dynamics on MATH Level 2 exhibit a pattern consistent with the Hard regime observed in our main experiments (Section 4.4):

- **Early Acceleration (Phase I):** The Normalized GRPO (standard, dashed blue line) establishes a clear performance lead early in training (steps 0–150), validating the benefit of adaptive step sizes in the initial high-variance, orthogonal regime.
- **Persistent Gap (Phase II):** A consistent accuracy gap (about 3 – 5%) is maintained throughout the middle stage of training (steps 150–400).
- **Late-Stage Convergence (Phase III):** Notably, towards the end of training (steps 450–500), the gap between the normalized method and the no_std baseline narrows significantly. This convergence strongly supports our theoretical analysis regarding the *High-Interference Regime*: as the model refines its representations for these complex problems, the loss of orthogonality introduces the benefits of normalization, causing the advantage to plateau.

These results confirm that the proposed local-curvature perspective and the identified training phases are robust across different datasets and difficulty levels.

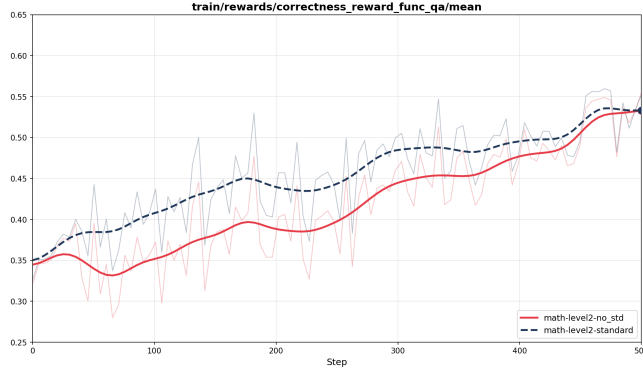


Figure 5. **Training dynamics on MATH Level 2 subset.** Similar to the GSM8K experiments, Normalized GRPO (standard) demonstrates faster initial convergence and maintains a lead for the majority of training. The narrowing gap in the final steps further evidences the impact of cross-prompt interference in the late training stages.

G. Details on Datasets and Training

G.1. Datasets

We evaluate our method on two distinct mathematical reasoning benchmarks to assess performance across varying scopes and difficulties:

GSM8K (Cobbe et al., 2021) This dataset serves as our primary benchmark for grade-school mathematical reasoning. To analyze the impact of normalization across difficulty regimes, we partition the training set into two subsets based on solution complexity:

- **Easy Split ($N = 4,695$):** Problems with lower reasoning complexity, serving as a low-variance control group.

- **Hard Split** ($N = 1,909$): Problems requiring multi-step reasoning with higher reward variance.

This partitioning is performed using `Qwen2-7B-Instruct` (Yang et al., 2024) as an evaluator model to classify problem difficulty.

MATH (Level 2) (Hendrycks et al., 2021) To evaluate generalization beyond grade-school arithmetic, we additionally employ the **Level 2** subset of the MATH benchmark. This subset consists of competition-style problems spanning diverse domains (e.g., algebra, geometry, number theory) with moderate difficulty, providing a testbed for robustness on varying problem structures.

G.2. Evaluation Metrics

Following standard protocols (Cobbe et al., 2021; Shao et al., 2024), we report sample accuracy (equivalent to greedy pass@1). This metric measures the fraction of problems for which the model’s generated answer exactly matches the ground truth. We employ standard regular expression matching to extract the final numerical answer from the model’s reasoning chain. For the orthogonality analysis in Section 4.1, we compute the cosine similarity between sentence-level embeddings of the penultimate hidden states.

G.3. Models

Our experiments utilize `Qwen2.5-Math-1.5B` (Yang et al., 2024) as the base policy model. We employ Low-Rank Adaptation (LoRA) (Hu et al., 2022) for parameter-efficient fine-tuning.

- **Policy Model:** `Qwen2.5-Math-1.5B`.
- **Training Configuration:** We apply LoRA to all linear layers with a rank $r = 64$ and alpha $\alpha = 128$.
- **Evaluator Model:** For dataset partitioning, we use `Qwen2-7B-Instruct` to ensure the classification capability exceeds the base model’s capacity.